

**PENYEDIAAN DAN PENCIRIAN KOMPOSIT NANO
4'-(4,4'-ISOPROPILIDENADIFENIL-1,1'-DILDIOKSI)
DIANILIN/ 4,4'- (4,4'-ISOPROPILIDENADIFENOKSIL)
BIS- (FTALIK ANHIDRIDA) POLIMIDA NIKEL
(BPADA-BAPP PI-NiNCs)**

NURU-DEEN JAJI

UNIVERSITI SAINS MALAYSIA

2023

**PREPARATION AND CHARACTERIZATION OF
4'-(4,4'-ISOPROPYLIDENEDIPHENYL-1,1'-DIYLDIOXY)
DIANILINE/ 4,4'- (4,4'-ISOPROPYLIDENEDIPHENOXY)
BIS- (PHTHALIC ANHYDRIDE) POLYIMIDE NICKEL
NANOCOMPOSITES (BPADA-BAPP PI-NiNCs)**

by

NURU-DEEN JAJI

**Thesis submitted in fulfilment of the requirements
for the degree of
Doctor of philosophy**

June 2023

DEDICATION

This thesis is affectionately dedicated to my beloved wife

Hajiya Rabi'atu Abubakar.

ACKNOWLEDGEMENT

Bismillahir-Rahamanir-Raheem. Alhamdu-lil laahi Rabbil aalameen. All praise be to Allah for blessing me with good health and the courage to successfully complete the PhD program. Peace and blessings be upon our Prophet, Nabi Muhammad sallahu alaihi wa sallam, our beloved and respected guidance to this ummah.

I would like to acknowledge and give my sincere gratitude to my supervisor Dr Muhammad Bisyrul Hafi Othman who made this work possible. His magnanimous guidance and advice carried me through all the stages of writing this thesis. I would also like to give special thanks to my co-supervisors; Associate Professor Dr Hooi Ling Lee and Associate Professor Dr Mohd Hazwan Hussin for their brilliant comments, suggestions, and guidance.

I would like to thank my field supervisor, Professor Dr Wan Ahmad Kamil Mahmood who has been a great mentor and source of tremendous support for me throughout my stay in Malaysia. Additionally, I wish to express my sincere gratitude to my mentor Professor Emeritus Dr David Hui of the University of New Orleans, United States of America.

I am indebted to my family who supported me over the last five years, my wife Hajiya Rabiatu Abubakar and my children; Fatimah Zarah, Muhammad Ridwan, Muhammad Mustapha, Abubakar Abba and Nana Khadijah for their constant love and affection.

Furthermore, my special appreciation goes to my good friends, Tuan Sherwyn Hamidon, Hajji Aminu Siraj, Muhammad Faisal Gassim, Muhammad Murwih Alidmat, Hajiya Halima Babamale, Abdullah Dauda Kida, and Sasitaran Munuganan. May Allah make all our affairs easy for us. Finally, I wish to express my deepest appreciation to the Federal Government of Nigeria for the award of TETFUND scholarship and the management of Federal College of Education Technical, for selecting me as a beneficiary of the scholarship.

TABLE OF CONTENTS

ACKNOWLEDGEMENT	ii
TABLE OF CONTENTS	iv
LIST OF TABLES	x
LIST OF FIGURES	xii
LIST OF SYMBOLS	xvi
LIST OF ABBREVIATIONS	xix
ABSTRAK	xxii
ABSTRACT	xxiv
CHAPTER 1 INTRODUCTION	1
1.1 Overview	1
1.2 Polyimide Nickel Nanocomposites (PI-NiNCs)	1
1.3 Problem Statement	3
1.4 Objectives of the Study	5
1.5 Research Hypothesis	5
1.6 Research Scope	7
1.7 Thesis Organization	9
CHAPTER 2 LITERATURE REVIEW	10
2.1 Overview	10
2.2 Nickel Nanoparticles (NiNPs)	10
2.2.1 Approaches in the Synthesis of NiNPs	11
2.2.1(a) Top-down Methods	11
2.2.1(b) Mechanical Milling	12
2.2.1(c) Laser Ablation	12
2.2.1(d) Thermal Decomposition	13
2.2.1(e) Nanolithography	13

2.2.1(f)	Sputtering Technique.....	14
2.2.2	Bottom-up Methods.....	15
2.2.2(a)	Sol-gel Technique.....	16
2.2.2(b)	Spinning Fabrication.....	16
2.2.2(c)	Chemical Vapour Deposition Technique (CVD).....	17
2.2.2(d)	Pyrolysis Technique.....	18
2.2.2(e)	Biosynthesis.....	19
2.2.3	Factors Affecting the Synthesis of NiNPs by Chemical Method.....	20
2.2.3(a)	Synthesis Medium.....	20
2.2.3(b)	Effect of Temperature.....	21
2.2.3(c)	Effect of Reactant Concentration.....	22
2.2.3(d)	Effect of pH.....	24
2.2.3(e)	Effect of Surface Modifier Concentration.....	24
2.2.3(f)	Effect of Reaction Time.....	27
2.3	Fabrication of Polyimide Ni Nanocomposites (PI-NiNCs) Thin Films.....	28
2.3.1	Synthesis of Polyimide.....	28
2.3.1(a)	Conventional One-Step Method.....	29
2.3.1(b)	Conventional Two-Step Method.....	30
2.3.1(c)	Conventional Three-Step Method.....	32
2.3.2	Fabrication of PI Nanocomposites Thin Films.....	33
2.3.2(a)	Ultraviolet Irradiation Technique.....	34
2.3.2(b)	In-situ Single Stage Technique.....	36
2.3.2(c)	Surface Modification Technique.....	37
2.3.2(d)	Direct Printing Technique.....	39
2.3.2(e)	Sputtering Technique.....	41
2.3.2(f)	Conventional Mixing Technique/ Sol-Gel Technique.....	43

2.4	Characterization and Properties of BPADA-BAPP Polyimide-Nickel Composites.....	45
2.4.1	Chemical Structure of PI Containing NiNPs	45
2.4.1(a)	Fourier Transform Infrared Analysis of PI-NiNCs.....	46
2.4.1(b)	Nuclear Magnetic Resonance (NMR) of polyimides	48
2.4.2	Chemical Stability of Polyimides	49
2.4.3	Morphology of Polyimide Containing NiNPs	51
2.4.3(a)	X-Ray Diffraction (XRD) Analysis of polyimide containing NiNPs.	52
2.4.3(b)	Field Emission Scanning Electron Microscopy (FESEM) Coupled with Energy Dispersive X-Ray (EDX) Analysis.....	53
2.4.4	Thermal Stability of PI Containing NiNPs	54
2.5	Kinetic Degradation of Polyimide Containing NiNPs.....	56
2.5.1	Determination of Kinetic Parameters of BAPP-BPADA Polyimide- NiNCs.....	56
2.5.1(a)	Flynn Wall Ozawa (F-W-O) Model.....	59
2.5.1(b)	Kissinger-Akahira-Sunose (K-A-S) Model.....	60
2.6	Electrochemical Study of PI Containing NiNPs.....	60
2.6.1	Cyclic Voltammetry Analysis of polyimide Containing NiNPs.....	62
2.6.2	Electrochemical Impedance of Polyimide Containing NiNPs.....	64
2.6.3	Dielectric Constant of Polyimide Containing NiNPs	65
2.7	Application of Polyimide Nickel Nanocomposites (PI-NiNCS)	67
2.7.1	Lithography Applications of PI-NiNCs.	67
2.7.2	Biomedical Applications of PI-NiNCs	68
2.7.3	Application of PI-NiNCs in The Fabrication of Electrodes.....	69
2.7.4	Applications of PI-NiNCs as Membrane Material.....	70
2.7.5	Dielectric Application of PI-NiNCs.....	71

2.7.6	Applications of PI-NiNCs in Light Emitting Diode (LED) Devices.....	72
CHAPTER 3 RESEARCH METHODOLOGY.....		74
3.1	Experimental Design.....	74
3.2	Raw Materials.	75
3.2.1	Raw materials used in Synthesizing NiNPs.	75
3.2.2	Raw materials used in Synthesizing BAPP- BPADA PI.	76
3.2.3	Solvents used in solubility studies.	77
3.3	Preparation of 4'-(4,4'-Isopropylidenediphenyl-1,1'-Diyldioxy) Dianiline/ 4,4'-(4,4'-Isopropylidenediphenoxy)-bis- (Phthalic Anhydride) Nickel Nanocomposite (BPADA-BAPP-NiNCs).	78
3.3.1	Nickel Nanoparticles (NiNPs) Synthesis via One-pot Solvothermal Method.....	78
3.3.2	Preparation of BAPA-BPADA PI Thin Films.	79
3.3.3	Preparation of Polyimide Nickel BAPP BPADA-NiNCs Thin Films	81
3.4	Characterization of NiNPs and BPADA-BAPPP PI NiNCs.....	81
3.4.1	Ultraviolet-visible (UV-Vis) Spectroscopy.	81
3.4.2	Fourier Transform Infrared (FT-IR) Analysis.	82
3.4.3	Proton (¹ H) Nuclear Magnetic Resonance (NMR)	83
3.4.4	X-Ray Diffraction (XRD) Analysis.	83
3.4.5	Transmission Electron Microscopy (TEM)	84
3.4.6	Field Emission Scanning Electron microscopy (FESEM) with Energy Dispersive X-ray (EDX) Analysis.....	84
3.4.7	Solubility.....	85
3.4.8	Thermogravimetric Analysis (TGA).....	86
3.4.9	Cyclic Voltammetry (CV) Spectroscopy	86
3.4.10	Electrochemical Impedance Spectroscopy (EIS).....	88
3.4.11	Dielectric Constant Analysis.....	88

CHAPTER 4 4 RESULTS AND DISCUSSION.....	90
4.1 Overview.....	90
4.2 Nickel Nanoparticles (NiNPs) Synthesis by One-pot Solvothermal Method.....	90
4.2.1 Effect of Reaction Parameters on the Formation of Nickel Nanoparticles	90
4.2.1(a) Effect of Reaction Temperature	91
4.2.1(b) Effect of pH Medium	92
4.2.1(c) The Influence of Concentration of Reactants.....	93
4.2.1(d) Effect of Reaction Time	95
4.2.2 UV-visible Spectra of Nickel Chloride (NiCl ₂ .6H ₂ O) and Nickle Nanoparticles NiNPs	96
4.2.3 Fourier Transform Infrared (FT-IR) Analysis of NiCl ₂ .6H ₂ O and NiNPs	97
4.2.4 Crystalline X-ray Diffraction and Transmission Electron Microscopic Analysis of Nickel Nanoparticles and Nickel Chloride.....	99
4.2.4(a) Crystalline X-ray Diffraction Analysis of Nickel Nanoparticles and Nickel Chloride	99
4.2.4(b) Transmission Electron Microscopic (TEM) Analysis of Nickel Nanoparticles and Nickel Chloride.....	101
4.2.5 Thermogravimetric Analysis (TGA) of NiCl ₂ .6H ₂ O and NiNPs.....	104
4.2.6 Proposed Reaction Mechanism for the Formation of NiNPs.....	106
4.3 Preparation of 4'-(4,4'-Isopropylidenediphenyl-1,1'-Diyldioxy) Dianiline/ 4,4'- (4,4'-Isopropylidenediphenoxy) Bis-(Phthalic Anhydride) Nickel Nanocomposite (BPADA-BAPP-NiNCs)	108
4.3.1 Preparation Consideration of BPADA-BAPP-NiNCs.....	108
4.3.2 Structure Conformation of BPADA-BAPP-NiNCs.....	111
4.3.2(a) FT-IR Analysis.....	111
4.3.2(b) H-NMR Analysis	112
4.3.3 Solubility of BPADA-BAPP-NiNCs	114

4.3.4	Morphology Analysis of PI-NiNCs	115
4.3.4(a)	X-ray Diffraction Analysis (XRD).....	115
4.3.4(b)	Field Emission Scanning Electron Microscopy (FESEM)/Energy Dispersive X-ray (EDX) Spectroscopy	116
4.3.5	Thermogravimetric Analysis (TGA) of BPADA-BAPP PI NiNCs Series.....	124
4.3.5(a)	Thermogravimetric Analysis.....	124
4.4	Non-Isothermal Kinetic Degradation of BPADA-BAPP PI-NiNCs	128
4.4.1	Activation Energy of BAPP-BPADA Polyimide-NiNCs	138
4.4.2	Lifetime Prediction of BAPP-BPADA PI-NiNCs	141
4.5	Electrochemical studies of PI-NiNCs	144
4.5.1	Cyclic Voltammetric (CV)Analysis of BPADA-BAPP PI- NiNCs	144
4.5.2	Electrochemical Impedance Spectroscopy of BAPP-BPADA PI NiNCs	149
4.5.3	Dielectric Constant of PI-Nickel Nanocomposites	152
CHAPTER 5 CONCLUSIONS.....		155
5.1	Conclusions.....	155
5.2	Recommendations for Future Studies	156
REFERENCES.....		158
LIST OF PUBLICATIONS		

LIST OF TABLES

		Page
Table 1.1	Synthesis prospects, properties, and applications of selected PI-NiNCs.	3
Table 2.1	Top-down techniques for the fabrication of Ni nanoparticles.....	12
Table 2.2	Selected bottom-up techniques for Ni nanoparticles production.....	15
Table 2.3	The “variation of amount of precursor and surfactant with NiNPs size (Guo <i>et al</i> , 2018).”	23
Table 2.4	Summary of ultraviolet techniques for the fabrication of PI nickel composites.	35
Table 2.5	Summary of in-situ fabrication techniques for PI-NiNCs.....	37
Table 2.6	Summary of surface modification techniques for the fabrication of nickel composites.....	39
Table 2.7	Summary of direct printing techniques for Ni on PI substrate.	40
Table 2.8	Summary of sputtering techniques fabrication of PI-Ni nanocomposites.	42
Table 2.9	Summary of sol-gel techniques for the fabrication of PI-NiNCs.	44
Table 2.10	“Solubility of PI Precursor (PAA) and PI in common solvents at room temperature (Othman <i>et al</i> , 2015).”	50
Table 2.11	Applications of PI-NiNCs in lithography.....	67
Table 2.12	Medical applications of PI-NiNCs.	68
Table 2.13	Application of PI-NiNCs as electrode materials.	69
Table 2.14	Selected PI-NiNCs in membrane applications.	70
Table 2.15	Dielectric applications of PI-NiNCs.....	71
Table 2.16	PIs containing Ni and their applications in light emitting diodes.....	73
Table 3.1	Chemical structure and physical properties of BAPP and BPADA.....	76

Table 3.2	Summary of the preparation of thin films of BPADA-BAPP PI and BPADA-BAPP PI-NiNCs series.	81
Table 3.3	Solubility test parameters of PI and BAPP-BPADA NiNCs 10 mL bottles at room temperature and 24 h.	85
Table 4.1	Solubility of BPADA-BAPP PI and BPADA-BAPP PI-NiNCs	114
Table 4.2	TGA properties of BPADA-BAPP PI and BPADA-BAPP PI NiNCs in nitrogen atmosphere.	126
Table 4.3	Values of E_a (kJ/mol) and their correlations by F-W-O method.	130
Table 4.4	The values of E_a (kJ/mol) and their correlations by K-A-S method.	135
Table 4.5	Average activation energies and average correlations for F-W-O and K-A-S methods.	139
Table 4.6	Results for the kinetic degradation parameter and the lifetime as a function of the service temperature of BPADA-BAPP PI and BPADA-BAPP PI NiNCs series.	142
Table 4.7	Specific capacitance comparisons for different BPADA-BAPP-NiNC series.	148
Table 4.8	Summary of resistance and capacitance of PI-NiNC series calculated from EIS circuit fitting.	152
Table 4.9	Dielectric constants of BPADA-BAPP PI-NiNCs series.	153

LIST OF FIGURES

	Page
Figure 2.1	Illustration of “thermal decomposition (Kobayashi <i>et al</i> , 2019).” 13
Figure 2.2	Illustration of the “nanolithography technique (Kumar <i>et al</i> , 2018).” 14
Figure 2.3	Illustration of “sol-gel procedure (Parashar <i>et al</i> , 2020a).”..... 16
Figure 2.4	Illustration of “spinning disc reactor (Khodashenas <i>et al</i> , 2015).” 17
Figure 2.5	Schematic diagram of “Chemical Vapour Deposition unit (Hoyos-Palacio <i>et al</i> , 2019).” 18
Figure 2.6:	Schematic diagram of “Pyrolysis technique for NiNPs synthesis (Das <i>et al</i> , 2019).” 19
Figure 2.7	Schematic representation of “Biosynthesis techniques for NiNPs production (Ali <i>et al</i> , 2020).” 19
Figure 2.8	Scheme of “Percentage conversion (% C) and temperature (T) for the decomposition of Ni(CO) ₄ in a reactor (Kholghy and Schumann, 2021).” 22
Figure 2.9	SEM images of NiNPs “generated using different modifiers (A) CTAB, (B) PEG-10000, (C) gelatin, (D) CTAB and PEG-10000, (E) CTAB and gelatin, and (F) commercial NiNPs (Jiang <i>et al</i> , 2013).” 26
Figure 2.10	Digital Images of “(a) 0.4 mol L ⁻¹ NaOH and (b) 0.7 mol L ⁻¹ NaOH from 0.5 h to 12 h of solutions after hydrothermal treatment Shao <i>et al</i> , (2018).” 28
Figure 2.11	Scheme of “photosensitive PIs prepared by conventional one-step method (Ghosh <i>et al</i> , 2012).” 30
Figure 2.12	Scheme of “colorless PI prepared by conventional two-step method (Yi <i>et al</i> , 2020).” 32
Figure 2.13	Scheme of “conventional three-step method for polyimide synthesis (Zhang <i>et al</i> , 2021).” 33
Figure 2.14	Scheme of “UV-irradiated nickel modification of polymer layer (Tamai <i>et al</i> , 2019).” 35

Figure 2.15	Scheme of “typical in-situ procedure for the fabrication of PI metal composite (Ramesh <i>et al</i> , 2009).”	36
Figure 2.16	Illustration of “direct printing of Ni on PI substrate (Chae <i>et al</i> , 2020).”	40
Figure 2.17	Schematic representation of “magnetron sputtering of Ni on substrate (Priyadarshini <i>et al</i> , 2014).”	41
Figure 2.18	Schematic representation of “products processed using sol-gel techniques (Catauro and Cipriotti, 2021).”	43
Figure 2.19	Image of “characteristic FT-IR absorption spectra of PIs (Mi <i>et al</i> , 2018).”	45
Figure 2.20	Image of “IR spectra of PI and NiO interaction (Aframehr <i>et al</i> , 2020).”	47
Figure 2.21	Image of a “typical ¹ H-NMR spectrum of PI (Hatami, 2017).”	48
Figure 2.22	Cross-sectional TEM images of “(a) PI film containing NiNPs (b) Enlarged image of NiNPs (Wu <i>et al</i> , 2017).”	51
Figure 2.23	Image of “X-RD patterns of PI loaded with NiNPs and annealing temperatures (Gao <i>et al</i> , 2020).”	53
Figure 2.24	Images of “FE-SEM and EDX of PI-NiNC (Stoica <i>et al</i> , 2020).”	54
Figure 2.25	Image of “TG-DSC curves of PI-Pristine and PI-NiNPs (Mu <i>et al</i> , (2010).”	55
Figure 2.26	Kissinger -Akahira-Sunose plots for “(a) PI, (b)PI+ 1 wt% MWCNT, and (c) PI + 1 wt% CNT (Nayak <i>et al</i> , 2018).”	56
Figure 2.27	Images of “magnetic hysteresis loops at various Ni content (Wang <i>et al</i> , 2020).”	61
Figure 2.28	“CV of PI containing Ni(OH) ₂ for various concentrations of glucose (Wang <i>et al</i> , 2019).”	63
Figure 2.29	“Nyquist plot for neat PI and PI containing Ni and inset equivalent circuit (Okafor and Iroh, 2021).”	64
Figure 2.30	Images of “(a) Dielectric constant (b) Dielectric loss evolution with temperature for various samples at frequency of 1 Hz (Hamciuc <i>et al</i> , 2021).”	66
Figure 3.1	Research flow chart	75
Figure 3.2	Summary of the synthesis of NiNPs via solvothermal technique.....	79

Figure 3.3	Schematic representation of equipment setup for preparation of polyamic acid.	80
Figure 3.4	Image of a typical electrochemical cell for CV experiment.	87
Figure 4.1	UV-Visible spectra of NiNPs at 100 °C, 150 °C, and 190 °C.	91
Figure 4.2	UV-Visible spectra of NiNPs at pH 9, pH 10, and pH 11.	93
Figure 4.3	UV-Visible spectra of NiNPs at 0.01M, 0.05 M, and 0.1 M.	94
Figure 4.4	UV-Visible spectra of NiNPs at a reaction time of 10 h, 16 h, and 24 h.	95
Figure 4.5	Overlay of the λ_{max} SPR of NiNPs and bulk nickel solution.	96
Figure 4.6	Overlay of FT-IR Spectra of EG, PEG, NiCl ₂ and NiNP.	97
Figure 4.7	XRD pattern with fitting of (a): NiCl ₂ .6H ₂ O (b): NiNPs	100
Figure 4.8	TEM (a) image of NiNPs at 20 KX. (b) Diameter distribution of 100 particles NiNPs using Image-J.	101
Figure 4.9	TGA and DTGA of NiNPs and NiCl ₂ .6H ₂ O.	105
Figure 4.10	Schematic representation of solvothermal reaction mechanism.	107
Figure 4.12	FT-IR of PI at various temperatures of imidization.	109
Figure 4.13	Degree of imidization of BPADA-BAPP PI.	110
Figure 4.13	FT-IR plots for BPADA-BAPP PI, BPADA-BAPP PI-NiNCs 1 wt.%, BPADA-BAPP PI-NiNCs 5 wt.% and BPADA-BAPP PI-NiNCs 10 wt.%.	111
Figure 4.14	H-NMR OF BPADA-BAPP.	113
Figure 4.16	XRD Pattern of BPADA-BAPP PI and BPADA-BAPP PI-NiNCs.	116
Figure 4.16	SEM monograms of film surface (a) BPADA-BAPP PI, (b) BPADA- BAPP PI NiNCs 1 wt.%, (c) BPADA-BAPP PI NiNCs 5 wt.% and (d) BPADA-BAPP PI NiNCs 10 wt.%.	117
Figure 4.17	SEM and EDX of (a) BPADA-BAPP PI, 0 wt.% (b) BPADA-BAPP PI NiNCs 1 wt.%, (c) BPADA-BAPP PI NiNCs 5 wt.% and (d) BPADA- BAPP PI NiNCs 10 wt.%.	121

Figure 4.18	TGA and DTG of BPADA-BAPP PI NiNCs series.....	124
Figure 4.19	F-W-O plots of (a) BPADA-BAPP PI, (b) BPADA-BAPP PI NiNCs 1 wt.%, (c) BPADA-BAPP PI NiNCs 5 wt.%, and (d) BPADA-BAPP PI NiNCs 10 wt.%.....	128
Figure 4.21	Plot of E_a against α by F-W-O method for BPADA-BAPP PI and BPADA-BAPP PI NiNCs series.	132
Figure 4.21	K-A-S plots of (a) BPADA-BAPP PI (b) BPADA-BAPP PI NiNCs 1 wt.%, (c) BPADA-BAPP PI NiNCs 5 wt.%, and (d) BPADA-BAPP PI NiNCs 10.....	133
Figure 4.22	Plot of E_a against α by K-A-S method for BPADA-BAPP PI and BPADA-BAPP PI NiNCs series.	136
Figure 4.23	Lifetime as function of the service temperature in presence of BPADA-BAPP PI NiNCs series in nitrogen atmosphere.	143
Figure 4.24	Cyclic voltammograms of PI-NiNCs with various loadings NiNPs (a) 0 wt.% Ni, (b) 1 wt.% Ni, (c) 5 wt.% Ni, and (d) 10 wt.% Ni.	144
Figure 4.25	Nyquist plot for BPADA-BAPP-NiNCs series.	149
Figure 4.26	Equivalent circuit fitting Nyquist plots for BPADA-BAPP PI-NiNCs series.	151

LIST OF SYMBOLS

%	Percent
%C	Percentage conversion
ΔT	$T_{(end)}-T_{(onset)}$
A	Exposed surface area of polymer film
C	Capacitance
cm^{-1}	Per centimeter
Cp	Specific capacitance
d	Thickness of polymer film
δ	Chemical shift
E_a	Activation energy
F	Faraday constant
h	Hour
I	Current
<i>Image-J</i>	Image analysis soft ware
k	Scan rate
kV	kilovolt
$k\alpha$	Electron from L-shell x-ray radiation
L	Thickness of polymer film
molL^{-1}	Mole per liter
n_a	Total number of imidizable groups
n_i	Number of imidized groups
nm	Nanometer
$^{\circ}\text{C}$	Degree Celsius
pH	Negative log of hydrogen ion concentration
Q	Charge on ion

R	Universal gas constant
R.E	Reference electrode
R ²	Average correlation
R _b	Polymer bulk resistance
S	seconds
T	Absolute temperature
t	Time in seconds
T _(10%)	Temperature corresponding to 10% weight loss
T _(5%)	Temperature corresponding to 5% weight loss
T _(end)	End temperature of degradation
T _(max)	Temperature at maximum weight loss
T _(onset)	Onset temperature of degradation
V	Voltage
W.E	Working electrode
w _f	Final weight after degradation
w _o	Initial weight at beginning of degradation
w _t	Actual weight at time <i>t</i>
w _t .%	Residue at T _(end)
w _t .%	Weight percent
Z _{imag}	Imaginary impedance
Z _{real}	Real impedance
α	Conversion factor
β	Heating rate
ε	Molar absorptivity
ε'	Dielectric constant
ε''	Dielectric loss
ε _o	Absolute permittivity of free space

λ	Wavelength
λ_{\max}	Absorbance maximum
τ	Time constant
ω	Angular frequency

LIST OF ABBREVIATIONS

¹ H-NMR	Proton nuclear magnetic resonance spectroscopy
6FDA	2,2-bis(3,4-dicarboxyphenyl) hexafluoropropane
6FDA	4,4'-(hexafluoroisopropylidene)diphthalic anhydride
AFM	Atomic force microscopy
BAPP	4,4'-(4,4'-isopropylidenediphenoxy) bis-(phthalic anhydride)
BPADA	4'-(4,4'-isopropylidenediphenyl-1,1'-diylidioxy) dianiline
BPDA	3,3',4,4'-biphenyltetracarboxylic dianhydride
BTDA	3,3',4,4' -benzophenone tetracarboxylic dianhydride
CBDA	Benzophenone tetracarboxylic acid dianhydride
CNF	Carbon nanofiber
CNT	Carbon nanotubes
cp	hexagonal close packed
CPI	Colorless polyimide
CTAB	Cetyltrimethylammonium bromide
CV	Cyclic voltammetry
CVD	Chemical vapour deposition technique
DC	Direct current sputtering
DMAc	N,N-dimethylacetamide
DMDEDA	3,3'-dimethyl-5,5'-diethyl-4,4'-diaminodiphenylmethane
DMF	Dimethylformamide
DMSO-d ₆	Dimethyl sulfoxide solvent in ¹ H-NMR
DTG	Differential thermogravimetry
EDX	Energy dispersive x-ray
EIS	Electrochemical impedance spectroscopy
ELD	Electroless deposition

fcc	face centered cubic
FESEM	Field emission scanning electron microscopy
FLS	Flashlight sintering
FT-IR	Fourier transform infrared spectroscopy
F-W-O	Flynn-Wall-Ozawa method
GPC	Gel permeation chromatography
K-A-S	Kissinger-Akahira-Sunose method
LBL	Layer by layer
MBA	N,N'- methylenebisacrylamide methanodibenzo [b, f] [1,5] diazocine
NiNCs	Nickel nanocomposites
NiNPs	Nickel nanoparticles
NMP	<i>N</i> -methyl-2-pyrrolidone
ODA	Oxydianiline
PAA	Polyamic acid
PANI	Polyaniline
PDMS	Polydimethylsiloxane
PEG	Polyethylene glycol
PET	Polyethylene terephthalate
PI	Polyimide
PI-NiNCs	Polyimide nickel nanocomposites
PI-NiNPs	Polyimide nickel nanoparticles
PMDA	Pyromellitic dianhydride
ppm	Parts per million
PTFE	Polytetrafluoroethylene
rGO	reduced Graphene Oxide
RF	Radio frequency sputtering
SEM	Scanning electron microscopy

SPI	Sulfonated Polyimide
TEM	Transmission electron microscopy
TEMDA	3,3',5,5'- tetraethyl-4,4'-diaminodiphenylmethane
TEOS	Tetraethyl orthosilicate
TGA	Thermogravimetric analysis
TG-DSC	Thermogravimetric-differential scanning calorimetry
THF	Tetrahydrofuran
TMMDA	3,3',5,5'-tetramethyl-4,4'-diaminodiphenylmethane
TMS	Tetramethyl silane
TOP	Trioctylphosphine
TTBDA	2, 8-bis (4-(tertbutyl) phenyl)-4, 10-diamino-6, 12-dihydro-5, 11-
UV	Ultraviolet
XPS	X-ray photoelectron spectroscopy
X-RD	X-ray diffraction

**PENYEDIAAN DAN PENCIRIAN KOMPOSIT NANO
4'-(4,4'-ISOPROPILIDENADIFENIL-1,1'-DILDIOKSI) DIANILIN/ 4,4'- (4,4'-
ISOPROPILIDENADIFENOKSIL) BIS- (FTALIK ANHIDRIDA) POLIMIDA
NIKEL (BPADA-BAPP PI-NiNCs)**

ABSTRAK

Kerja ini memberi tumpuan kepada penyediaan dan pencirian, 4'-(4,4'-isopropilidenedifenil-1,1'-diyildioksi) dianilina/ 4,4'- (4,4'-isopropilidenedifenoksi) bis- (phthalik anhidrida) poliimida nikel nanokomposit (BPADA- PINiNC BAPP). Pada mulanya, Nikel Nanopartikel (NiNPs) berjaya disediakan melalui sintesis “one-pot” solvoterma. Pembentukan NiNP telah disahkan oleh Ultraviolet– visible (UV-Vis) dengan λ_{\max} pada 265 nm, puncak Fourier Transform Infrared (FT-IR) pada 630 cm^{-1} (regangan Ni-O), indeks satah X-ray Diffraction (XRD) ((100), (111), (200), (220)), diameter zarah purata 49 nm pada imej Mikroskop Elektron Penghantaran (TEM) dan keputusan Analisis Termogravimetrik (TGA) dengan lebih daripada 97% sisa selepas degradasi selesai pada 800 °C. NiNP ini telah berjaya dimasukkan ke dalam matriks BPADA-BAPP PI dengan teknik pengadunan larutan. FESEM dan EDX mengesahkan morfologi dan komposisi unsur Ni diperhatikan meningkat kepada 1.05%. Siri BPADA-BAPP PINiNCs menunjukkan sifat kebolehprosesan yang baik dalam pelarut aprotik kutub. Dalam kajian kinetik degradasi haba melalui kaedah F-W-O dan K-A-S, korelasi purata (R^2) bagi tenaga pengaktifan (E_a) adalah lebih besar daripada 0.97 menunjukkan kesesuaian yang agak baik. Keputusan yang diperolehi untuk kedua-dua model menunjukkan peningkatan dalam kestabilan dengan peningkatan dalam pemuatan NiNP. Kajian elektrokimia BPADA-BAPP PI-NiNC telah berjaya dijalankan. Spektroskopi Impedans Kapasiti spesifik yang diperolehi untuk siri polimida dan polimida tulen bertambah baik daripada 7.68×10^{-14} kepada

3.70×10^{-9} , manakala kekuatan bertambah baik daripada 5.68×10^{-11} kepada 1.85×10^{-8} dan nilai pemalar dielektrik bertambah baik daripada 2.94 kepada 627.1. PI-NiNC BPADA-BAPP didapati meningkatkan sifat kekonduksian apabila kandungan nanopartikel nikel meningkat. Nanokomposit fabrikasi dengan kestabilan terma yang tinggi, pemalar dielektrik rendah dan kekonduksian elektrik yang dipertingkatkan mempunyai potensi aplikasi dalam lapisan perantara dielektrik, mikroelektronik, superkapasitor dan peranti optoelektronik.

PREPARATION AND CHARACTERIZATION OF 4'-(4,4'-ISOPROPYLIDENEDIPHENYL-1,1'-DIYLDIOXY) DIANILINE/ 4,4'-(4,4'-ISOPROPYLIDENEDIPHENOXY) BIS- (PHTHALIC ANHYDRIDE) POLYIMIDE NICKEL NANOCOMPOSITES (BPADA-BAPP PI-NiNCs)

ABSTRACT

This work focusing specifically on the preparation and characterization of the 4'-(4,4'-isopropylidenediphenyl-1,1'-diyldioxy)dianiline/4,4'-(4,4'-isopropylidenediphenoxy) bis- (phthalic anhydride) polyimide nickel nanocomposites (BPADA-BAPP PINiNCs). Initially, Nickel Nanoparticles (NiNPs) were successfully prepared by one-pot solvothermal synthesis. The formation of NiNPs was confirmed by ultraviolet– visible (UV-Vis) with λ_{\max} at 265 nm, Fourier transform Infrared (FT-IR) peak at 630 cm^{-1} (Ni-O stretching), X-ray diffraction (XRD) indexed planes (100), (111), (200) and (220), average particle diameter of 49 nm at Transmission Electron Microscopes (TEM) image, and thermogravimetric analysis (TGA) results with more than 97% of residues after degradation was completed at 800 oC. This NiNPs were successfully incorporated into BPADA-BAPP PI matrix by solution blending technique. Field Emission Scanning Electron Microscope (FESEM) and Energy Dispersive X-Ray Analysis (EDX) was confirmed the morphology and elemental composition has increased to 1.05%. The series of BPADA-BAPP PINiNCs showed good processability properties in polar aprotic solvents. In the kinetic thermal degradation studies through the Flynn-Wall-Ozawa (F-W-O) and Kissinger-Akahira-Sunose (K-A-S), the average correlation (R^2) of the activation energy (E_a) are greater than 0.97 suggesting a relatively good fit. The results obtained for both models indicated increase in stability with increase in NiNPs loading. The specific capacitance obtained for pure polyimide and polyimide series improved from 7.68×10^{-14} to 3.70×10^{-9} , while capacitance improved from 5.68×10^{-11} to 1.85×10^{-8} and dielectric

constant values improved from 2.94 to 627.1. The BPADA-BAPP PI-NiNCs were found to enhance the conductivity properties as the content of nickel nanoparticles increased. The fabricated nanocomposites with high thermal stability, low dielectric constant and enhanced electrical conductivity have potential applications in interlayer dielectrics, microelectronics, supercapacitors, and optoelectronic devices.

CHAPTER 1

INTRODUCTION

1.1 Overview

The utilization of NiNPs in PI system does not only require knowledge of the application requirements, but a fundamental understanding of the chemical structure and properties relationships. These areas are addressed in the term of aromatic PI derived from BPADA and BAPP monomers in the presence of NiNPs. The subtle variation in the structure of the polymeric backbone and nano particle composition in PI matrix have tremendous effect on the properties of the PI-NiNCs. Therefore, the first part of this chapter reviews the status, research gap, and potential, as well as the application of the PI-NiNCs. Consequently, the limitations of the PI regarding its synthesis, preparation and compatibility are highlighted. A synergistic approach is proposed by focusing on four main objectives and several hypotheses regarding its performance in PI activities are discussed. Next, the chapter justifies the reason for why some of the raw materials, reagents and parameters are chosen. The chapter ends with an overall summary of what is presented in this dissertation.

1.2 Polyimide Nickel Nanocomposites (PI-NiNCs)

The incorporation of Nickel nanoparticles into the polyimide (PI) backbone resulting in the changes that occurred in the structural, thermal, kinetic, and electrochemical properties of the pure PI and the nickel nanocomposites. Nickel fillers in PI nanocomposites have been widely synthesized for their excellent magnetic properties and conductivity. “Yoonessi *et al*, (2015) described the synthesis of oriented hybrid nickel tethered graphene PI resin nanocomposite with enhanced magnetic

properties and conductivity.” “Dorneanu *et al*, (2015) reported the fabrication of nanocomposite fibers from electrospon solution by incorporating different amounts of nickel nanoparticles, which correlated with photophysical changes in the presence of different loads of nickel nanoparticles.” “Chen *et al*, (2015) narrated the preparation and properties of novel superparamagnetic well dispersed waterborne polyurethane nickel nanocomposites.” “Okafor and Iroh, (2021) revealed the enhancement of electrochemical properties of porous graphene PI composite electrode by the electrode deposition of nickel oxide on to the electrode.” The nickel nanoparticles greatly improved the thermal behavior and mechanical properties of the nanocomposite. Recently, “Nam *et al*, (2021) reported the thermal stability of PI/Ni-grid produced by a novel technique for the generation of flexible and high-performance heaters.”

The fabrication of PI-NiNCs is essential because neat polyimides exhibit high heat stability, high resistivity, and excellent breakdown voltage. “Wu *et al*, (2017) noted that, their inability to exhibit electric and thermal conductivity limits their further application as conductive devices.” Therefore, considerable efforts have been made in this work to improve the PI processability to enable the incorporation of NiNPs into the PI matrix. Several research groups extensively “reported the mechanical, thermal and electrochemical properties of gold Godard *et al*, (2020)”, “silver Lee *et al*, (2021)”, “platinum Szabo *et al*, (2020)” and other precious metals. However, these precious metals are expensive whereas Ni is less costly and will serve the purpose of improving the thermal and electrochemical properties of the PI substrate. The synthesis prospects, targeted properties, and practical applications of selected PI-NiNCs are presented in **Table 1.1**.

Table 1.1: Synthesis prospects, properties, and applications of selected PI-NiNCs.

Polyimide-Nickel Composite	Enhanced properties	Targeted applications	References
PI/CNT/Ni foams	Charge transfer	Electronic/sensing devices	(Gao <i>et al.</i> , 2020)
PI/carbon fiber/Ni-Co	UV absorption performance	Microelectronic systems	(Li <i>et al.</i> , 2022)
PI/Ni micro patterns	High transmittance	Heaters	(Nam <i>et al.</i> , 2021)
PI/graphene/NiNPs	Electromagnetic shielding	Shielding material	(Yin <i>et al.</i> , 2021)
PI/graphene/NiO	Ionic diffusion	Supercapacitors	(Okafor and Iroh, 2021)
PI/Ni ions	Zeta potential	Photonic crystals	(Deng <i>et al.</i> , 2020)
PI/PANI/Ni-Co-Fe-P	Heat transfer efficiency	Aerospace devices	(Wang <i>et al.</i> , 2020)

Polyimide matrix with a variety of incorporated nickel constituents such as Ni foams, NiO, NiNPs, Ni-Co have recently been employed to fabricate PI-Ni containing nanocomposites. These nanocomposites exhibit enhanced properties including electromagnetic shielding, charge transfer, high transmission as well as ionic diffusion. The enhanced properties of the nanocomposites predispose them to a wide-ranging application inclusive of sensing devices, shielding materials, super capacitors, as well as aerospace devices.

1.3 Problem Statement

The synthesis of NiNPs via solvothermal oleylamine route requires standard air-free procedures coupled with space and time-consuming experimental setup. Whereas traditional wet methods require several stages of synthesis protocol and produced hcp rather than stable fcc phase. In hydrothermal route, highly reactive and flammable sodium phosphide, sodium hypophosphite and red phosphorus have been used making the synthesis potentially explosive. These drawbacks are minimized by

the utilization of one-pot solvothermal method via environmentally friendly and economically viable chemicals.

Despite the industrial and technological applications of PIs, their processing is limited by their high glass transition temperature and lack of solubility in most organic solvents. Similarly, the applications of PIs are limited because they lack thermal and electrical conductivity. The addition of metal nanoparticles is necessary to offer electrical and thermal transmission as in the current fabrication of BPADA-BAPP-Ni nanocomposites.

Among the significant parameters to establish the thermal stability of PI nanocomposites is to study the E_a in relation to the commencement of thermal degradation transformation. However, the thermal degradation kinetics and lifetime prediction of BPADA-BAPP-NiNCs is rarely available in literature. The kinetic behavior and thermal stability of the BPADA-BAPP-NiNCs has been expected to depend on the composition and the E_a values obtained from the kinetic degradation studies. Hence the need to study the degradation kinetics of the BPADA-BAPP-NiNCs.

Amidst the notable challenges of PI nanocomposites are relatively low ionic conductivity at ambient temperature as well as insufficient ionic conductivity for practical applications in all solid-state devices. Recent studies show that Ni based composites exhibit high specific capacitance and excellent power characteristics due to a variety of charge storage mechanisms. Therefore, NiNPs are used in this study due to its high capacitance and low toxicity.

1.4 Objectives of the Study

The aim of this research is to fabricate BPADA-BAPP-NiNCs and investigate the combined intrinsic properties of the organic and inorganic components. The main objectives of the study were:

1. To investigate the influence of reaction temperature, pH of solution, the concentration of reactants, and reaction time on the synthesised NiNPs, through one-pot Solvothermal method.
2. To fabricate a series of BPADA-BAPP PI thin films containing NiNPs via solution blending.
3. To evaluate the contribution of NiNPs loading on the thermal stability of BPADA-BAPP PI-NiNCs thin films using non-isothermal kinetic degradation.
4. To investigate the thermal, processability and electrochemical properties of BPADA-BAPP PI-NiNCs thin films.

1.5 Research Hypothesis

The primary hypothesis was that the synthesized NiNPs through one-pot solvothermal route could avoid NiNP instabilities by introduction of capping agent such as polyethylene glycol (PEG). Moreover, non-toxic precursor and modifier materials were employed in the synthesis. The successful synthesis of NiNPs will be confirmed by UV-Visible spectroscopy with expected characteristic Ni absorbance band, FT-IR absorption is expected to show a peak for Ni-O stretching mode, XRD expected to show four characteristic diffraction peaks corresponding to the indexed planes characteristic of NiNPs.

The secondary hypothesis was that the NiNPs will be successfully reinforced into fully imidized BPADA-BAPP PI through conventional mixing method. The FT-IR spectrum will be expected to confirm that the membrane is fully imidized by investigating the absorption peak for (C-N-C) peak. The presence of Nickel nanoparticles is expected to be observed using XRD analysis and confirmed by SEM analysis and EDX. The solubility test of BPADA-BAPP PI-NiNCs will be conducted successfully using common solvents to prove the current hypothesis.

The tertiary hypothesis was that the kinetic parameters of the BPADA-BAPP PI-NiNCs can be determined using Fynn-Wall-Ozawa (F-W-O) and Kissinger-Akahira-Sunose (K-A-S) non-isothermal models, leading to lifetime prediction. The F-W-O and K-A-S methods are used to quantify the activation energy (E_a). These methods may be used to calculate E_a without knowledge of the reaction mechanism. Because this is not predicated on any assumptions about the temperature integral, the findings can be more precise. Therefore, the approach is a free model methodology for determining the dependency of the effective E_a on (α) the conversion factor. Moreover, the approach is appropriate for the kinetic comprehension of the thermogravimetric complex reaction data obtained. The Kissinger-Akahira-Sunose method is used to determine the E_a of the solid-state reaction. The K-A-S model has the benefit of not requiring the heat degradation response mechanism to be determined in advance to derive the E_a .

Finally, the fourth hypothesis was that the conductivity of PI containing nickel nanoparticles will increase with increasing nickel loading when investigated via cyclic voltammetry and electrochemical impedance spectroscopy techniques. The influence of Nickel nanoparticle towards electrochemistry are investigated through the effect of NiNPs loading. Furthermore, by increasing the content of nickel nanoparticles,

conductivity also can be improved as the inter particle distance decreases. Therefore, the conductivity of PI-NiNCs will be dependent on the concentration of the nickel nanoparticles in the PI matrix. The conductivity current will be investigated by a contacting sensor using cyclic voltammetry (CV). The current is expected to increase proportionally with voltage and voltammogram will change from symmetrical to asymmetrical. Addition of NiNPs to the PI enhance the conductivity current. The electrochemical results obtained will be used to generate specific capacitance, capacitance and dielectric constant values for the pure PI and PI-nickel nanocomposite series.

1.6 Research Scope

The study has certain limitations in the following areas: in the synthesis of NiNPs, the optimization of reaction parameters was limited to few variations such as reaction temperature was limited to 100, 150 and 190 °C in line with the economics of production. At temperature below 100 °C reaction cannot lead to the formation of products due to low frequency of collisions. Similarly, the desired NiNP were formed at 190 °C. This was considered the optimized value of temperature because it will require less material and energy based on economic considerations as the lowest temperature to obtain products. The pH values were limited to 9, 10 and 11. Hence the choice of pH 9 as the optimized value as the lower pH at which products were obtained for economic viability. The optimized concentration of reactants was set at 0.1 M, values below this were too dilute for the formation of products whereas higher values of concentration will not be economical friendly. Reaction time was optimized at 24 h because below this duration NiNPs will not be formed. Therefore, 24 h was considered the most cost-effective option with respect to economics of production.

The second limitation is the amount of NiNPs used in the fabrication of BPADA-BAPP PI. The minimum amount of NiNPs in the composites is 1% and the maximum amount of NiNPs composite is 10%. Using the minimum amount of NiNPs of 1% makes it difficult to analyse the products with Scanning Electron Microscopy (SEM) analysis, X-Ray Diffraction (XRD) analysis and other characterization techniques. The maximum amount of NiNPs in the composite is limited to 10% because PI films containing more than 10% will be brittle and easily break.

In the kinetic degradation studies of PI-NiNCs, several other multiple non-isothermal heating methods can be used to calculate the E_a such as F-W-O, Kissinger, H-Met, C-Red, Mac-T, Friedman, Van Krevelen, and many more are favoured for the same purpose. However, in this study only two methods were employed namely, F-W-O and K-A-S methods due to it independent toward the mechanism type of solid state the degradation.

The electrochemical properties of BPADA-BAPP PI-NiNCs were investigated using electrochemical impedance spectroscopy (EIS) and cyclic voltammetry (CV). The conductivity of BPADA-BAPP PI-NiNCs was studied using different content of NiNPs loading. However, several other electrochemical techniques are available for the study of PI composites such as amperometry, conductometry, electrogravimetry and coulometry which have not been used in this work. The solvent used to dissolve the film in this study is chloroform, whereas other solvents with lower boiling point and volatility can be used.

1.7 Thesis Organization

This thesis consists of five (5) chapters. **Chapter 1** describes a concise introduction of the thesis. It provides an overview of the research work, followed by problem statement, objectives of the study, hypothesis, research scope and an outline of the thesis structure.

Chapter 2 covers detailed overview and review of literature on the subject matter of synthesis of NiNPs, preparation of PI containing NiNPs, characterization, and properties of PI-NiNCs, kinetic degradation of PI-NiNCs, electrochemical studies of the nanocomposites and related literature on similar research studies were reported.

Chapter 3 describes experimental design, raw materials, preparation of NiNPs, fabrication of PI-NiNCs, and their characterization. The description of equipment and experimental techniques conducted in this research were similarly reported.

Chapter 4 reports the results and discussion of NiNPs synthesis, fabrication of PI-NiNCs, kinetic degradation studies of BPADA-BAPP PI-NiNCs and the electrochemical investigation of PI-NiNCs.

Chapter 5 reports the conclusion drawn from this research and equally presents the recommendations for future studies on the current subject matter.

CHAPTER 2

LITERATURE REVIEW

2.1 Overview

This dissertation is a contributing research segment with regards to the preparation and characterization of thermosetting PI-NiNCs films. Therefore, this chapter is divided into seven sections namely; overview, synthesis of nickel nanoparticles, fabrication of PI-nickel nanocomposite thin films, characterization, and properties of BPADA-BAPP PI-nickel composites as well as kinetic degradation of PIs containing nickel nanoparticles. There will be a review of the development in synthesis and structure/properties modification of PI NiNCs films as published in literature. Since this study began with the preparation of NiNPs the first section starts with the recent studies on the top-down synthesis techniques involving the breakdown of materials to nano size, and bottom-up synthesis techniques the assembly of nanoparticles from precursors in the solvothermal and physical synthesis of NiNPs. Consequently, the latest survey on principles and techniques on fabrication of PI-NiNPs thin films has been discussed in detail. The final section will review the literature survey on the latest principles and theories in kinetic degradation and electrochemical study of PI and screen the current application on PI-NiNCs.

2.2 Nickel Nanoparticles (NiNPs)

“NiNPs possess a great potential as a catalyst in reactions, propellant, and sintering additive, in coatings plastics and fibers (Hill *et al*, 2019).” Due to its relative abundance in the earth crust, “Ni is more cost-effective than most of the metals in use as catalyst (Bian *et al*, 2017)”. Nickel is mostly found in ores and sometimes found

free in nature. Nickel can be alloyed with metals especially chromium, iron, molybdenum, tungsten as well as other metals to form corrosion resistant alloys.

“The electrical conductivity of Ni enables its use in several applications (Behroozfar *et al*, 2020).” “NiNPs can be used as nanofluids in high purity, ultra-high purity, passivated, coated, and distributed forms (Wang *et al*, 2019).” Therefore, the selection of the procedures in NiNPs synthesis such as “green chemical approaches (Marzun *et al*, 2017)” to “physical methods (Menezes *et al*, 2014)” are important in the overall applications of NiNPs. Various reports confirm the applications of NiNPs in the “fields of nanotechnology (Oujja *et al*, 2018)” , “science and biomedical sciences (Yao *et al*, 2015).” “The specific advantages of Ni nanoparticles as catalyst in reactions are discuss, in comparison to other magnetic nanoparticles (Kobayashi *et al*, 2019).”

2.2.1 Approaches in the Synthesis of NiNPs

2.2.1(a) Top-down Methods

“Breaking down bulk materials into nanoscale sizes is part of top-down synthesis techniques using chemical, electrochemical, and mechanical grinding protocols (Park *et al*, 2005).” “It include mechanical grinding of coarse particles to nanosized particles, electrochemical deposition of nanoparticles from a metal electrode (Pandey *et al.*, 2019)” “mechanical milling, laser ablation (Gonzalez-Martinez *et al.*, 2019)” “nanolithography, thermal decomposition, and sputtering (Tanjeem *et al*, 2022).” The main advantages of top-down techniques include well developed techniques, fabrication of products with controlled shape and size as well as cost effectiveness. “The disadvantages are limitations in nanofabrication tools and difficulty in the manipulation of tools to produce desired wavelength of light (Aryal *et*

al, 2019).” Selected top-down approaches for the synthesis of NiNPs are presented in **Table 2.1**.

Table 2.1: Top-down techniques for the fabrication of Ni nanoparticles

Top-down Technique	Application of Ni nanoparticles	Reference
Lithography	Biomedical	(Lami et al, 2020)
Chemical etching	Catalyst	(Heilmann et al, 2020)
Laser ablation	O2 evolution	(Wawrzyniak et al, 2020)
Mechanical milling	Material softening	(Liu et al, 2019)
Ball milling	Catalyst for CO2 hydrogenation	(Yuan et al., 2015)
Sputtering	Magnetic biocatalyst	(Bussamara et al, 2013)
Robust catalytic reactions	Catalyst	(Li and Zeng, 2018)
Plasma processing	Electro catalyst	(Kim et al, 2013)

2.2.1(b) Mechanical Milling.

Mechanical milling is the most common method of generating diverse nanoparticles among the different top-down methods. Mechanical milling is employed during synthesis and post-annealing of nanoparticles to grind various elements in an inert environment. “Mechanical milling is impacted by plastic deformation, which contributes to a given shape, whereas fracture reduces particle size and cold welding enhances particle size (Molnárová *et al*, 2018).”

2.2.1(c) Laser Ablation.

Laser ablation synthesis is a method for creating nanoparticles from various liquids. Nanoparticles are created by irradiating a metal submerged in a liquid solution with a laser beam, which condenses the plasma plume and produces nanoparticles. In the synthesis of nanoparticles, laser ablation synthesis is a dependable process as well

as an alternative to chemical metal reduction. “This method provides a stable synthesis of nanoparticles in organic solvents and water without requiring stabilizing or capping agent (Oujja *et al*, 2018).”

2.2.1(d) Thermal Decomposition.

Heat generated by endothermic chemical breakdown destroys the bonds in the substance in this approach. The temperature at which an element chemically decomposes is referred to as its decomposition temperature. As a result, “the nanoparticles are produced by decomposing the metal at its decomposition temperature, resulting in a chemical process that produces the nanoparticles (Yao *et al*, 2015).” **Figure 2.1** shows a scheme of thermal decomposition techniques to produce NiNPs.

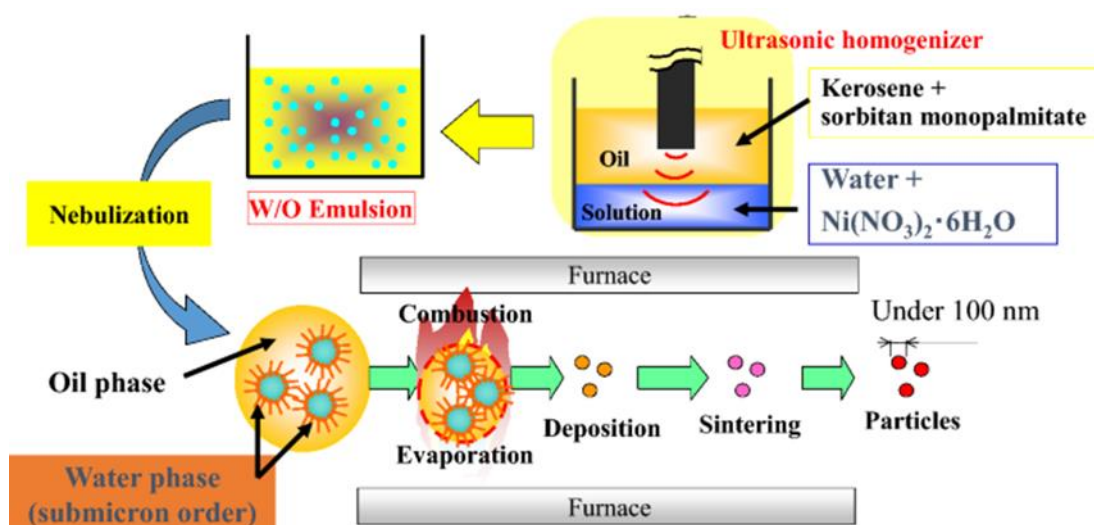


Figure 2.1: Illustration of “thermal decomposition (Kobayashi *et al*, 2019).”

2.2.1(e) Nanolithography.

Nanolithography is an approach to fabricate nanomaterials with one dimension in the range of 1 to 100 nm. These techniques include nanoimprint, optical, multiphoton, electron-beam, and scanning probe nanolithography. Nanolithography is

a method of printing the necessary shape or structure on a substrate that is susceptible to light and extracts part of the material selectively to obtain the required shape and structure. “Nanolithography enables the production of a single nanoparticle to a cluster of nanoparticles with the desired shape and size (Mary *et al*, 2011).” The disadvantages of these techniques are the requirements of complex equipment and the associated cost. **Figure 2.2** shows an illustration of the nanolithography technique to produce nanoparticles.

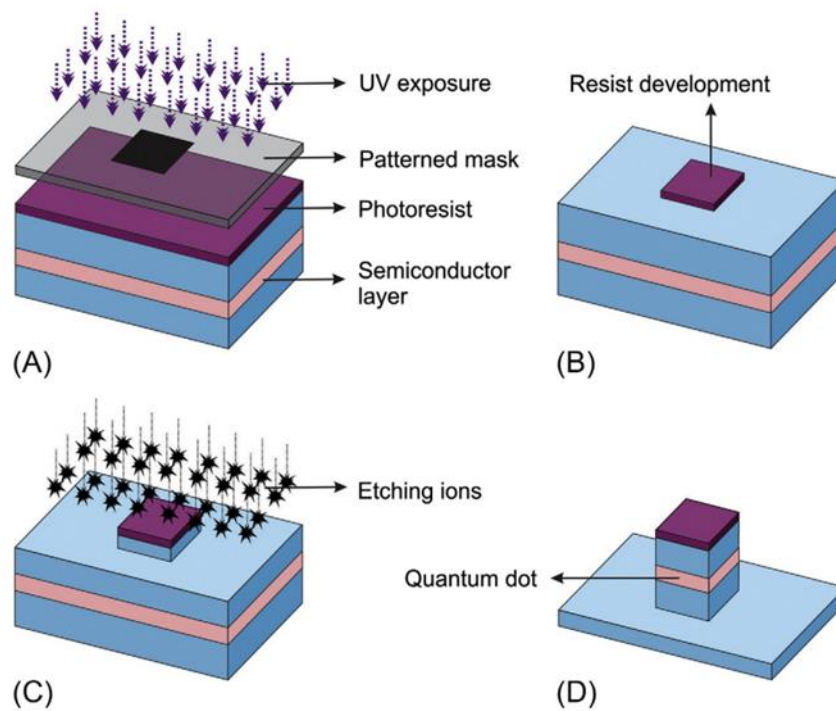


Figure 2.2: Illustration of the “nanolithography technique (Kumar *et al*, 2018).”

2.2.1(f) Sputtering Technique.

In the sputtering technique, the deposition of nanoparticles on a surface occurs by the ejecting particles as they collide with ions. “Sputtering is the deposition of a thin layer of nanoparticles followed by annealing (Rodrigues *et al*, 2019).” The shape and size of the nanoparticles are determined by the substrate type, thickness of the layer, duration of annealing, and operating temperature.

2.2.2 Bottom-up Methods

Bottom-up methods include the use of metallic oxides and metallic salts as reaction precursors. Using a suitable solvent and reducing agent, these salts or oxides are finally converted to metallic nanoparticles. The dispersal mode, shape, and dimensions of the nanoparticles may be altered using these procedures by adjusting the concentrations of the precursor and reducing agent, the pH, temperature, heating duration, and the kind and choice of the stabilizing agent. “Several bottom-up approaches include spitting, solvent-gel, gas evaporation, and coprecipitation techniques and plant-mediated synthesis (Chen and Wu, 2000).” The advantages of bottom-up techniques are the fabrication of nanostructures with less defects and homogeneous chemical composition of the products. “The limitations of these approaches include the requirement of capital-intensive equipment (Abid *et al*, 2022).” **Table 2.2** shows some selected bottom-up techniques for the synthesis of Ni nanoparticles.

Table 2.2: Selected bottom-up techniques for Ni nanoparticles production

Bottom-up Technique	Application Ni nanoparticles	Reference
Chemical vapour deposition	Antimicrobial	(Chaudhary et al, 2019)
Sol-gel process	Superparamagnetic material	(Li et al. 2012)
Laser pyrolysis	Advanced functionalized material	(McKeown et al, 2012)
Spray-pyrolysis	Water splitting	(Raj et al, 2022)
Atomic condensation	Electro catalyst	(Fadil et al, 2014)
Pulse ablation	Antibacterial activity	(Khashan et al, 2016)
Aerosol process	Enhanced electro catalytic activity	(Khalid et al, 2018)

2.2.2(a) Sol-gel Technique.

The sol- a colloidal solution of particles floating in a liquid phase- and the gel- a solid macromolecule immersed in a solvent- are used in this approach. Many metallic nanoparticles can be manufactured using this process, which is the most popular bottom-up method due to its simplicity. “This is a wet-chemical process using a chemical solution comprising an integrated system of discrete particles as the precursor (Li and Zhang, 2017).” Metal oxides and salts are the typically used precursors in the sol-gel process. The precursor is then dispersed in a host liquid either by sonication, shaking, or stirring and the resultant system contains a liquid and a solid phase. Various methods such as filtration, sedimentation, and centrifugation are used to recover the nanoparticles. **Figure 2.3** shows an illustration of the sol-gel technique.

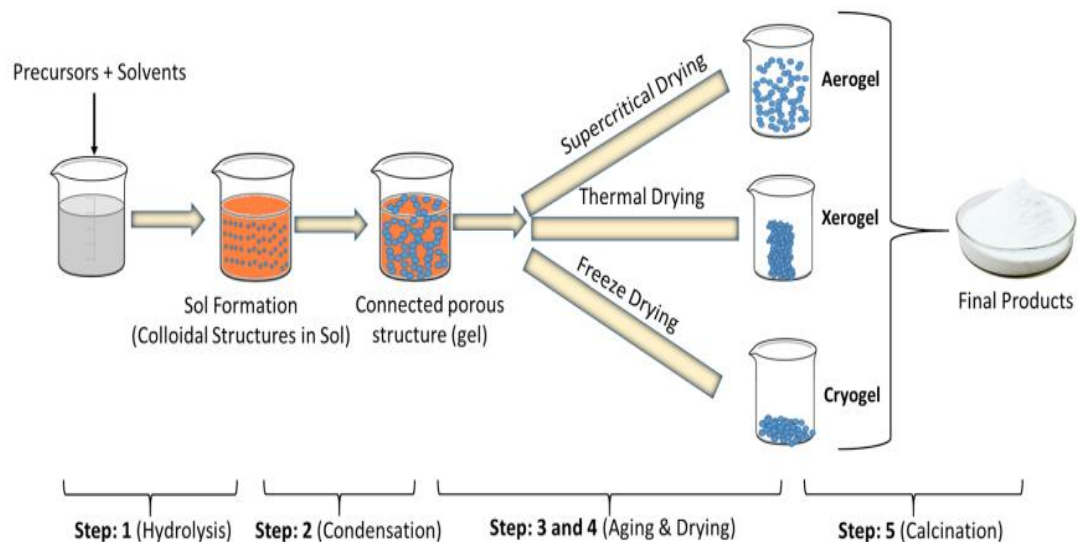


Figure 2.3: Illustration of “sol-gel procedure (Parashar *et al*, 2020a).”

2.2.2(b) Spinning Fabrication.

In this technique, the synthesis of nanoparticles is carried out by a spinning disc reactor. The rotating disc contains an inner chamber where the physical parameters such as temperature are controlled. The reactor is filled with inert gases or

nitrogen to remove oxygen and avoid chemical reactions. The liquid precursor and water are pumped into the chamber and the disc is rotated at a different speed. “The spinning allows the atoms or molecules to fuse together and are precipitated, collected, and dried (Manzano *et al*, 2017).” The characteristics of the synthesized nanoparticles are determined by various operating parameters such as the disc rotation speed, liquid flow rate, location of feed, disc surface, and liquid/precursor ratio. **Figure 2.4** shows an illustration of a spinning disc fabrication technique.

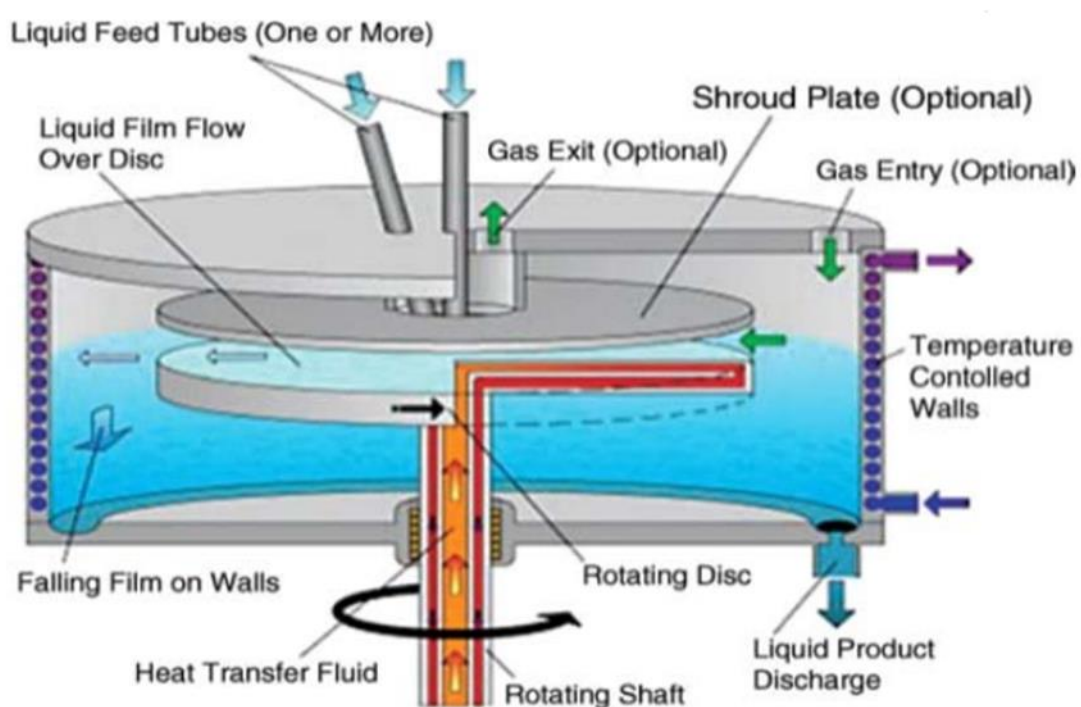


Figure 2.4: Illustration of “spinning disc reactor (Khodashenas *et al*, 2015).”

2.2.2(c) Chemical Vapour Deposition Technique (CVD).

In this technique, a thin film of gaseous reactants is deposited onto a substrate. The combination of gas molecules occurs in the reaction chamber at ambient temperature. The heated substrate then undergoes a chemical reaction with the combined gas. A thin film of products is deposited on the substrate surface which is recovered and used. “In CVD the influencing factor is the substrate temperature

(Riikonen *et al*, 2012).” **Figure 2.5** shows a schematic diagram of a chemical vapour deposition unit for growing carbon nanotubes using NiNPs as catalyst.

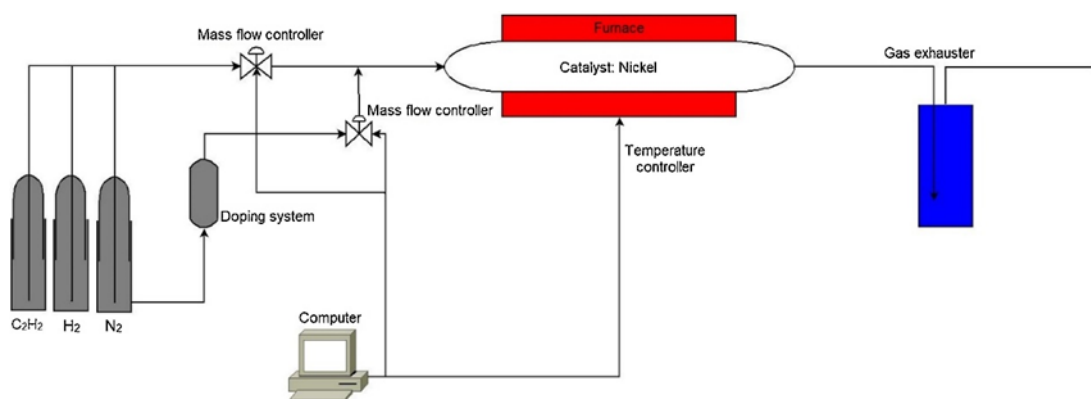


Figure 2.5: Schematic diagram of “Chemical Vapour Deposition unit (Hoyos-Palacio *et al*, 2019).”

Chemical vapour deposition advantages include the production of uniform, highly pure, hard, and strong nanoparticles. The disadvantages of CVD are highly toxic gaseous by-products and the prerequisite of unique equipment for the synthesis.

2.2.2(d) Pyrolysis Technique.

Pyrolysis is the most employed technique in industries for large scale production of nanoparticles. The precursor is burned in a flame. The liquid or vapor precursor is fed into the furnace through a small hole where it burns at high pressure. “The nanoparticles are then recovered from the combustion or by-product gases (Clemente *et al*, 2018).” In some furnaces, laser and plasma are used rather than a flame to produce high temperature enabling easy evaporation. **Figure 2.6** is a schematic diagram for the synthesis of highly dispersed nickel catalyst by pyrolysis technique. Pyrolysis employs simple methodology, high yield with economic efficiency as well as a continuous operation.

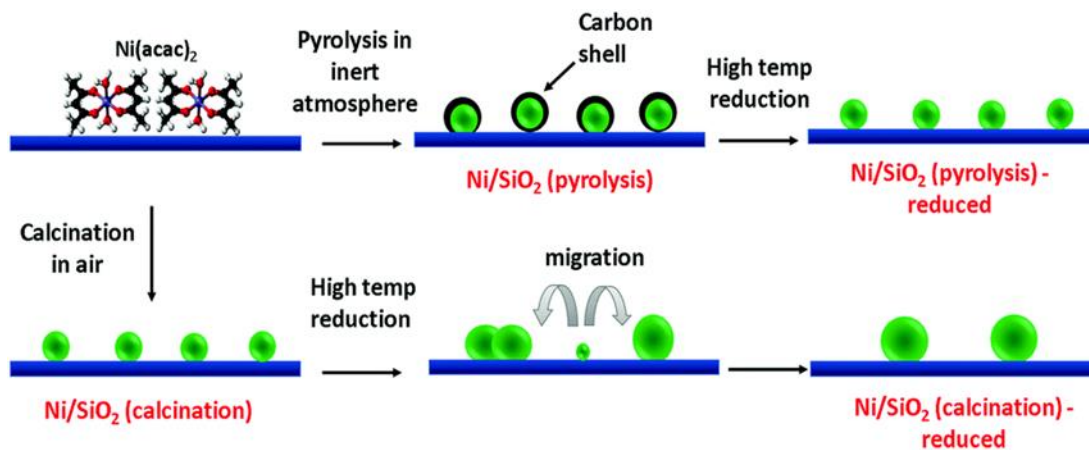


Figure 2.6: Schematic diagram of “Pyrolysis technique for NiNPs synthesis (Das *et al*, 2019).”

2.2.2(e) Biosynthesis.

Figure 2.7 shows a schematic illustration of the biosynthesis of nickel nanoparticles using plant parts and microorganisms as precursors.

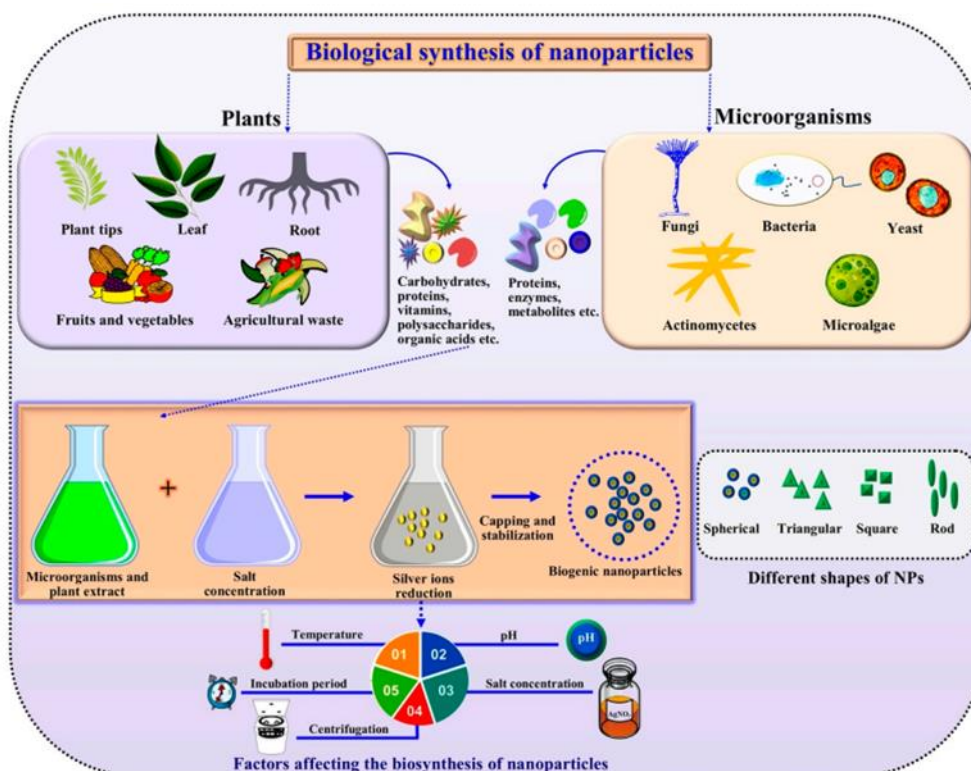


Figure 2.7: Schematic representation of “Biosynthesis techniques for NiNPs production (Ali *et al*, 2020).”

These techniques are used in the synthesis of nanoparticles that are nontoxic and biodegradable. Biosynthesis is a renewable and environmentally friendly approach. “Plant extracts, bacteria, fungi, together with the precursors are used to produce nanoparticles rather than conventional chemicals for bio-reduction and capping purposes (Alsammarraie *et al*, 2018).” The nanoparticles synthesized by this approach are unique and possess enhanced properties that comply with the requirements of biomedical applications

2.2.3 Factors Affecting the Synthesis of NiNPs by Chemical Method.

As has been reported, the major factors affecting the synthesis of NiNPs are dependent on the nanoparticles size and the average particle size distribution which determines the subsequent applications of the NiNPs. The critical factors to choose include selection of the reaction media, the physical parameters of reaction, for instance temperature, reactant concentration, pH of the reaction media, the nature of the reaction as well as reaction time.

2.2.3(a) Synthesis Medium

The synthesis medium determines the ultimate particle size and size distribution at the end of the reaction. The synthesis media of nanoparticles includes firstly, bulk aqueous phase medium, this method enables easy separation of the particles, facile treatment to obtain pure products, and ease of scaling-up the production. “Khanna *et al*, (2009) synthesized NiNPs in aqueous medium.” They obtained nanoparticles with an average particle distribution of 10-15 nm. Their study illustrates convenient, simple, and technologically powerful techniques for the synthesis of NiNPs. Secondly, Microemulsion method, in this technique

microemulsion nanoreactor is used to synthesize the nanoparticles. “Alymov *et al*, (2019) synthesized NiNPs using the microemulsion nanoreactor technique to obtain nanoparticles with controlled particle size and pyrophoricity of the NiNPs.” Thirdly, “Sol-gel techniques involve a colloidal solution of solids suspended in a liquid phase and a solid macromolecule submerged in a solvent (Karatutlu *et al*, 2018).” “Xu *et al*, (2014) reported the phase structure of the obtained NiNPs were hcp and fcc structure for those pyrolyzed at 250-350 °C and 750 °C respectively.” The hcp NiNPs were 5 to 20 nm in diameter and fcc were 7 to 35 nm. The hcp and fcc NiNPs showed significant magnetic properties.

2.2.3(b) Effect of Temperature

Temperature is the most significant reaction parameter in the kinetic control of reactions for the synthesis of nanoparticles. Temperature is generally an important parameter for polymerizations, thermal decomposition, and precipitation reactions. However, the effect of temperature is not significant for sol-gel and reduction reactions. The formation of NiNPs occurs in three stages namely: Nucleation, growth, and agglomeration. The size of the nanoparticles formed depends on the relative kinetics of these three steps. “De Jesús *et al*, (2018) synthesized NiNPs via direct thermal decomposition of nickel acetate tetra hydrate by varying the initial concentration of the precursor during pyrolysis.” They heated non-isothermally different initial concentrations of the precursor in argon atmosphere at 10 °C/min from ambient temperature to 500 °C, the NiNPs were readily obtained. The size distribution of the NiNPs was 40 to 140 nm. **Figure 2.8** shows the percentage conversion (% C) and temperature (T) of Ni(CO)₄ in a reactor.

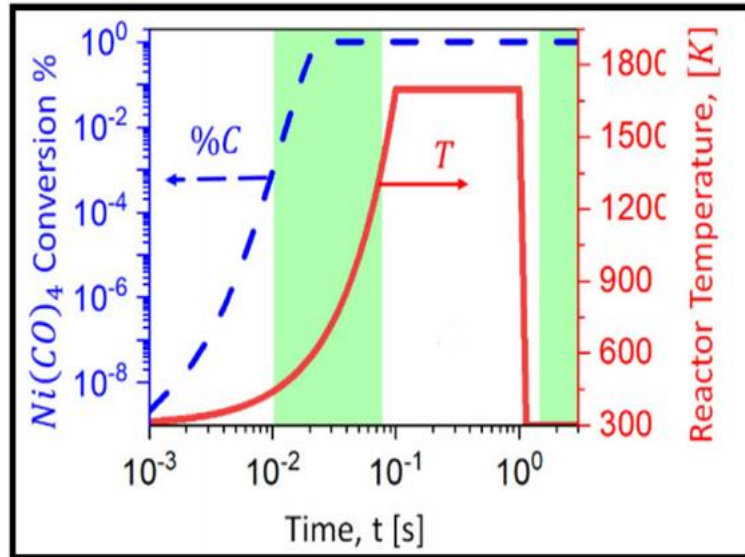


Figure 2.8: Scheme of “Percentage conversion (% C) and temperature (T) for the decomposition of $\text{Ni}(\text{CO})_4$ in a reactor (Kholghy and Schumann, 2021).”

As shown in **Figure 2.8** the percentage conversion increased with increasing temperature. At low temperatures and early stages of sintering surface diffusion is the dominant sintering medium to produce NiNPs. However, grain boundary diffusion dominated as the reaction progressed at higher temperatures. This agrees with “molecular dynamics simulations of noble metal nanoparticles (Kholghy and Schumann, 2021).”

2.2.3(c) Effect of Reactant Concentration

Reactant concentration is an important parameter for the control of NiNPs shell thickness or size. The ultimate particle size consists of two stages firstly, the formation of nuclei by the reactants and secondly, collision between nuclei to create the final particle size. The first step is the rate determining step which is then followed by the second step of growth. Generally, “an increase in concentration of reactants leads to higher collisions and consequently greater number of nuclei are formed giving rise to

smaller sized particles (Chaudhuri and Paria, 2012).” A slow reaction rate favors the formation of uniform coating hence a low reactant concentration is more favorable for NiNP production.

“Guo *et al*, (2018) discussed the synthesis of size-dependent monodispersed NiNPs.” They reported that the concentration of precursors affects the rate of nucleation and growth of the nanoparticles subsequently altering the mass transfer. Accordingly, NiNPs of different sizes were prepared by varying the ratio of nickel acetylacetonate (Ni(acac)₂) precursor and surfactant trioctylphosphine (TOP). Their investigation showed that increasing the precursor concentration produced larger particles, while increasing the surfactant quantity yielded smaller sized NiNPs. They produced a table showing the variation of precursor amount and the quantity of surfactant as provided in **Table 2.3**. The table contains detailed amount of precursor Ni(acac)₂ and surfactant TOP, together with the resulting NiNPs having different sizes. Increasing the amount of TOP was observed to yield smaller NiNP sizes. The table clearly shows the significance of precursor and surfactant concentration in the synthesis of NiNPs.

Table 2.3: The “variation of amount of precursor and surfactant with NiNPs size (Guo *et al*, 2018).”

Precursor Ni(acac) ₂ (g)	Surfactant (TOP) (mL)	NiNP sizes (nm)
0.4578	3	27.4
0.3818	3	18.8
0.3032	3	13.3
0.3032	6	8.9
0.3032	9	4.9

2.2.3(d) Effect of pH

The effect of pH on the synthesis of NiNPs is mainly determined by the attendant reaction mechanism. The effect is more pronounced when hydrogen or hydroxyl ions are involved in the reaction. The pH of the media is especially important for precipitation and reduction reactions. In a redox couple the half-cell reduction is significantly affected by the pH of the media. Consequently, the reaction leading to the formation of NiNPs can be controlled by manipulating the pH of the media. Furthermore, the amount of surface modification is equally controlled by turning the pH of the media.

“Roy and Bhattacharya, (2014) reported the synthesis of size-controlled, polymer protected NiNPs.” They stated that the maintenance of proper pH is the critical condition for the synthesis of NiNPs, contrary to that Ni will be converted to Ni^{2+} . The average particle diameter of NiNPs decreased when the ratio of Ni(II)/polymer was decreased as all the samples were maintained at the pH range of 11 to 12. “Wu *et al*, (2012) discussed the production of size-controlled NiNPs via electroless plating technique.” They concluded that the average particle size increased by increasing pH values and that suitable alkalinity of the solution was necessary to avoid fast precipitation of $\text{Ni}(\text{OH})_2$. They successfully synthesized size-controlled NiNPs with an average diameter of 9 to 20 nm.

2.2.3(e) Effect of Surface Modifier Concentration

The concentration of surface modifier plays a critical role in the synthesis of NiNPs due to size control and morphology of the nanoparticles. Surface modifiers containing ions are adsorbed on the particle surface to generate uniform charge. Reducing the agglomeration tendency of the particles leads to the production of